



Impact Assessment of Cyclone Amphan on Agriculture Over Parts of West Bengal Using Remote Sensing

PRABIR KUMAR DAS*¹, TANUMI KUMAR¹, SOUMYA BANDYOPADHYAY¹, SAON BANERJEE²

¹Regional Remote Sensing Centre-East, NRSC, New Town
Kolkata - 700 156, West Bengal, India

²Department of Agrometeorology and Physics, Bidhan Chandra Krishi Viswavidyalaya
Mohanpur - 741 252, West Bengal, India

Received: 08-04-2021

Accepted: 25.11.2021

Super-cyclone Amphan caused a devastating impact on agriculture in West Bengal. The present study aims at identifying the agricultural areas affected due to cyclone Amphan led water inundation in twelve selected districts of Gangetic West Bengal. The Sentinel 1 data of both pre- and post-cyclonic periods were analyzed to obtain the inundation area. Subsequently, the multi-temporal Landsat 8 datasets of 2019 and 2020 from April to June were analyzed to assess the crop conditions existing during the pre-cyclonic period. Both the layers were intersected to estimate the district-wise inundated agricultural areas along with the crop conditions. The post-cyclone water inundation was highest (43408 ha.) in Purba Medinipur. Among the inundated agricultural area, the standing crop including both growing and mature was significantly higher than harvested crop area. The validation with the ground-based information shows that the proposed approach was able to detect the crop conditions existing during the pre-cyclonic period efficiently with more than 90% accuracy. Hence, the same methodology may be adopted for assessing the crop damages caused due to cyclone induced inundation.

(Key words: Amphan, Landsat 08, Sentinel 1, Inundation, Crop assessment, Cyclone)

Over the past two centuries, tropical cyclones have been responsible for the deaths of about 1.9 million people worldwide. Under the climate change scenario, the intensity and frequency of tropical cyclones have considerably increased (Houghton *et al.*, 2001; Solomon *et al.*, 2007). Tropical cyclones at the landfall region cause extensive damage to human settlements, mangroves and wildlife habitats in the forest areas due to flat topography and tidal ingress. About one-tenth of the global tropical cyclones occur in the Bay of Bengal, of which one-sixth had landfall on the Sundarbans coast.

The 'Extreme Severe Cyclonic Storm' Amphan formed over the Bay of Bengal and made landfall between Digha (West Bengal) and Hatiya islands (Bangladesh) on May 20, 2020 (Mitra *et al.*, 2020). The regions of Purba Medinipur, North and South 24 Parganas, Howrah, Hugli and Paschim Midnapore were affected by the concomitant heavy rainfall (Das, 2020). Amphan claimed about 100 lives and more than 10 million people had been affected. The cyclone had caused massive damage to field crops and uprooting of trees, along with an adverse effect on water and power

supply. After the Phailin cyclone that had hit the Bengal-Odisha coast in 2013, Amphan is said to be the strongest tropical cyclone to hit the coast.

Remote sensing satellite data, like Landsat, provide vital information for monitoring a disaster like that of a cyclone, assessing its aftermath and helps in strategic decision-making for pre-disaster and post-disaster occurrences (Nandi *et al.*, 2017; Sarker *et al.*, 2019; DeVries *et al.*, 2020; Sajjad *et al.*, 2020). Both optical and microwave data have been utilized to delineate flooded and non-flooded areas in disaster-affected regions. Synthetic Aperture Radar (SAR) data for crisis mapping has provided an advantage over optical sensors by enabling data collection despite cloud cover, during all the seasons, day or night (Islam *et al.*, 2010; Hoque *et al.*, 2011; Dumitru *et al.*, 2015; Musa *et al.*, 2015; Clement *et al.* 2018; Notti *et al.*, 2018; Ezzine *et al.*, 2020).

The present study aims at identifying the agricultural areas affected due to Amphan led water inundation using Landsat 08 OLI and Sentinel 1 satellite images.

*Corresponding author: E-mail: prabirkumar_d@nrsc.gov.in

MATERIALS AND METHODS

The present study was conducted over twelve districts of West Bengal which were mainly affected due to cyclone Amphan, viz., Bankura, Howrah, Hugli, Kolkata, Jhargram, Paschim Barddhaman, Purba Barddhaman, Paschim Medinipur, Purba Medinipur, North 24 Parganas, South 24 Parganas and Nadia. The shaded area in Fig. 1 depicts the study area. The districts were selected by analyzing the track of the cyclone Amphan.

The datasets used in this study include Landsat 8 Operational Land Imager (OLI) L1 multispectral data with 30 m spatial resolution, Sentinel-1A and land use/land cover maps from Natural Resource Census (NRC) at 1:50,000 scale. Sentinel-1A C-band vertical transmitting with horizontal receiving (VH) polarization data of two dates covering both pre-cyclonic (16th May, 2020) & post-cyclonic (22nd May, 2020) periods were used in the study for delineating surface water bodies and water inundated areas. Landsat 8 OLI images of 2019 and



Fig. 1. Study area

2020 covering the study area during 1st week of April to 1st fortnight of June were downloaded from the USGS online archive Earth Explorer (<https://earthexplorer.usgs.gov/>). Total of 44 Landsat OLI images were used in the present study. The Land use/land cover maps were used to obtain the agricultural area mask.

Sentinel Ground Range Detected (GRD) data of 16th May, 2020 and 22nd May, 2020 were downloaded from Copernicus data hub (<https://scihub.copernicus.eu/dhus/#/home>). The datasets were pre-processed through a series of steps for obtaining the backscattering image, *i.e.*, sigma naught (σ_0). The major steps include application of orbit file, thermal noise removal, border noise removal, calibration for obtaining backscattering images, followed by speckle filtering and terrain correction (Fillipponi, 2019). The pre-processing of microwave datasets was carried out using SNAP (Sentinel Application Platform) software. Further processing was carried out using the VH (vertically transmitted and horizontally received) polarized backscattering images. A thresholding approach was adopted with values less than -16.0 dB to delineate the surface water pixels for both the pre- and post-cyclonic periods (Fig. 2). Both the surface water pixels layers were utilized to prepare the Amphan led inundation layers.

The L1 Landsat images were subjected to radiometric calibration using ENVI (Environment for Visualizing Images) software for converting the

calibrated digital numbers into absolute units of at-sensor spectral radiance. The radiometrically calibrated images were then atmospherically corrected using the Fast Line-of-sight Atmospheric Analysis of Spectral Hypercubes (FLAASH) model, setting the parameters of scene centre location, sensor type, flight data and time according to the header files of images, and setting the parameter of the atmospheric model as tropical. This was followed by the elimination of cloud contaminated pixels using the blue band reflectance thresholding approach.

The normalized difference vegetation index (NDVI) was calculated using red and near infra-red reflectance bands. The image tiles with path & row of 138-44, 138-45, 139-44 and 139-45, respectively were mosaicked to develop fortnightly NDVI images covering the study area for individual years using ERDAS (Earth Resources Data Analysis System) Imagine software. The cloud cover areas (data gaps) during the present year were filled by linear interpolation using both present (2020) and previous years (2019) data. The resultant NDVI images for the present year belong to 06th -13th April, 22nd -29th April, 08th -15th May, 24th -31st May and 09th -16th June. The agricultural area mask (NRC 1:50,000) was utilized to restrict the study within the agricultural area only. The multi-temporal NDVI based crop growth profiles were studied for identifying the crop growth stages existing during the pre-cyclonic period. The logical decision

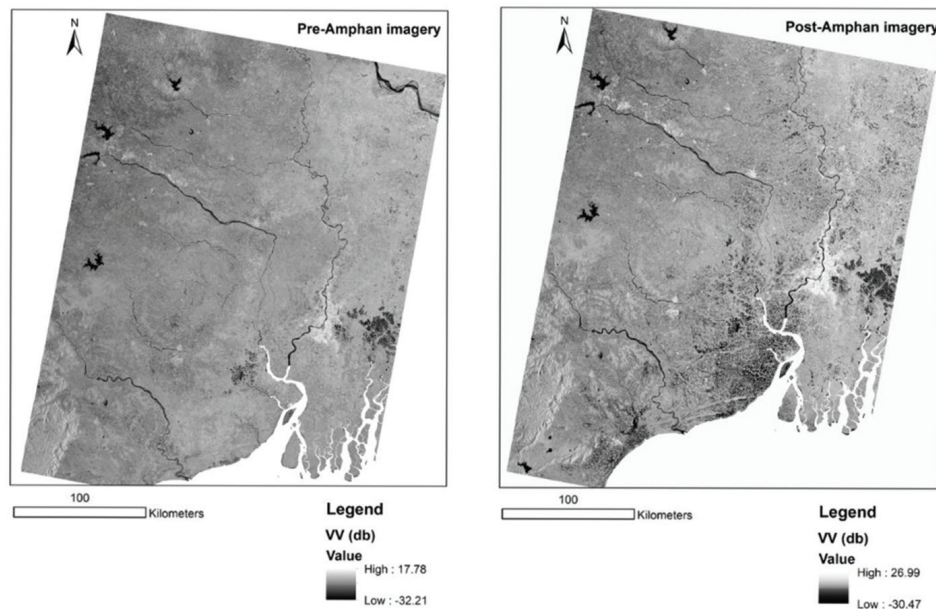


Fig. 2. Microwave images of pre- and post-cyclonic stages

rules were applied to categorize the agricultural area into three classes, viz., standing growing crop, standing matured crop and already harvest crop. The decision rules are provided in Table 1.

Further, the inundation layer derived from Sentinel-1A was overlaid over classified agricultural areas and district-wise crop conditions were estimated using ERDAS Imagine software. The severity of the damage due to inundation depends on the existing crop stages during the cyclonic event, which is the standing matured cropland > standing growing cropland > harvested cropland.

RESULTS AND DISCUSSION

The agricultural area under different study districts is represented in Fig. 3. Among all the study districts, the maximum area under agriculture was found in Bankura district with an area of 423729 ha, whereas it was minimum in Kolkata, i.e., 612 ha (Table 2).

By studying the NDVI profiles derived from multi-temporal Landsat images, different decision rules were developed to estimate the crop conditions during pre-cyclonic phase. It was hypothesized that during

cyclonic events the standing mature crops were under maximum risk, whereas the already harvested crops are under lower danger. The standing crops were under intermediate risk zone. Due to lack of information, the present study did not address the situations where crops were harvested, but the produces were still in the field. The distributions of different crop categories for different districts are given in Fig. 4 a & b. It was found that in most of the districts, except Nadia and Purba Medinipur, the proportions of standing crops were higher in comparison to mature crops in the field. In the case of Bankura and Paschim Barddhaman, the standing crop occupied more than 60% of the agricultural area, whereas in other districts it was generally more than 50%. The proportions of mature crops in the field were 30-40% in a majority of the districts, except Kolkata, Paschim Barddhaman, South 24 Parganas and Bankura with less than 30% contribution of standing crop. On the other hand, a significant portion, i.e., > 30% of agricultural area, under harvested cropped area was found in districts like Paschim Barddhaman, South 24 Parganas and Paschim Medinipur.

A threshold-based approach with values less

Table 1. NDVI based logical criteria

Case	Criteria	Category
1	NDVI peak during 06-13 April and NDVI during 22-29 April < 0.5 and NDVI during 08-15 May < 0.25	Harvested Crop
2	NDVI peak during 06-13 April and NDVI during 22-29 April < 0.5 and NDVI during 08-15 May > 0.25	Standing Mature Crop
3	NDVI peak during 22-29 April and NDVI during 08-15 May > 0.40	Standing Green Crop
4	NDVI peak during 22-29 April and NDVI during 08-15 May < 0.40	Standing Mature Crop
5	NDVI peak during 08-15 May	Standing Green Crop
6	NDVI peak during 24-31 May	Standing Green Crop
7	NDVI peak during 09-16 June and NDVI during 08-15 May < 0.25	Harvested Crop
8	NDVI peak during 09-16 June and NDVI during 08-15 May > 0.25 & < 0.40	Standing Mature Crop
9	NDVI peak during 09-16 June and NDVI during 08-15 May > 0.40	Standing Green Crop

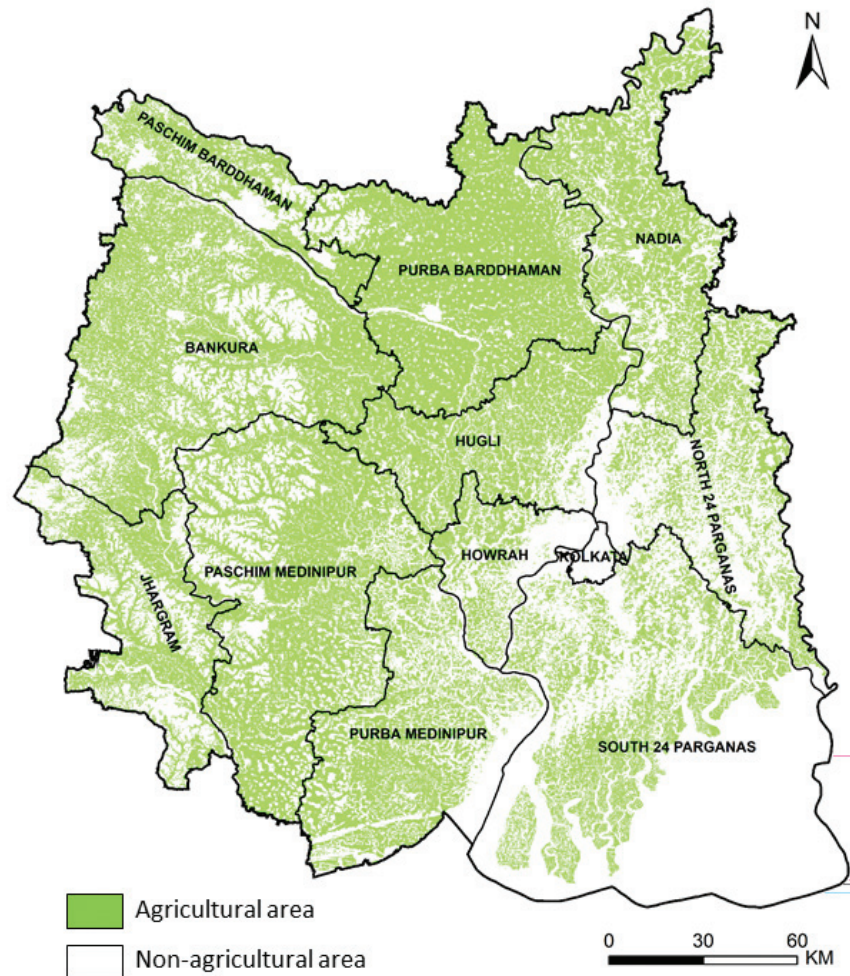


Fig. 3. Spatial distribution of agricultural area in the study area

Table 2. Area under agricultural area for selected districts

District	Area under agriculture (ha)
Bankura	423729
Kolkata	612
Howrah	54046
Purba Medinipur	201855
Paschim Barddhaman	105922
North 24 Parganas	134975
Jhargram	153213
Nadia	232776
South 24 Parganas	209499
Hugli	202570
Paschim Medinipur	380750
Purba Barddhaman	407641

than -16.0 dB backscatter coefficient was adopted for detecting the inundated area due to cyclone Amphan. The distribution of inundated area in different study districts are represented in Fig. 5. The area under inundation were around 277 ha, 6564 ha, 43408 ha, 999 ha, 14121 ha, 2290 ha, 7244 ha, 14031 ha, 8252 ha, 9865 ha, 8149 ha and 3754 ha for Kolkata, Howrah, PurbaMedinipur, Paschim Barddhaman, North 24 Parganas, Jhargram, Nadia, South 24 Parganas, Hugli, Paschim Medinipur, Purba Barddhaman and Bankura, respectively. Hence, highest inundation due to cyclone Amphan was found in Purba Medinipur, followed by North and South 24 Parganas.

The inundated and crop condition layers were utilized to derive information regarding the crop conditions that prevailed in the inundated area. The

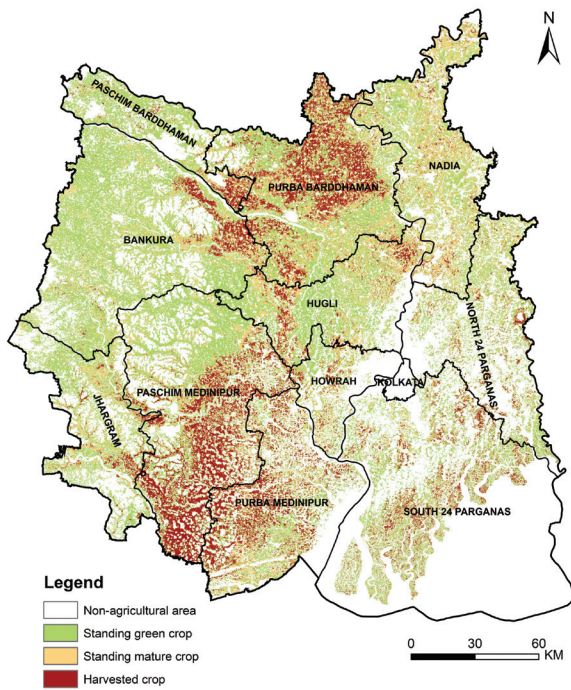


Fig. 4a. Spatial distribution of crop categories in the study area

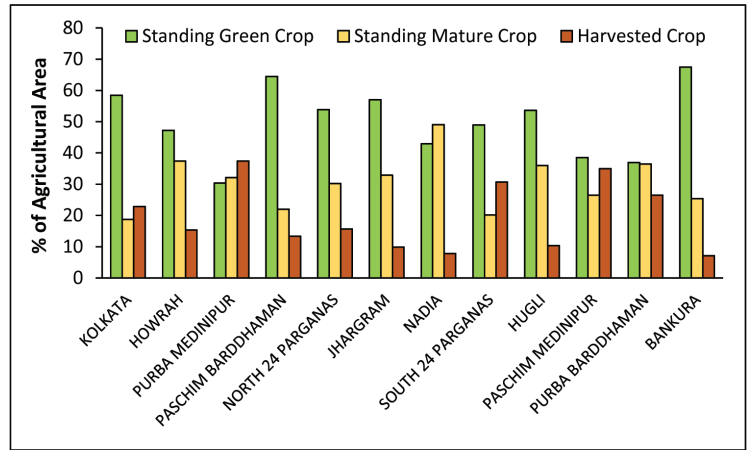


Fig. 4b. Percentage crop category for different districts

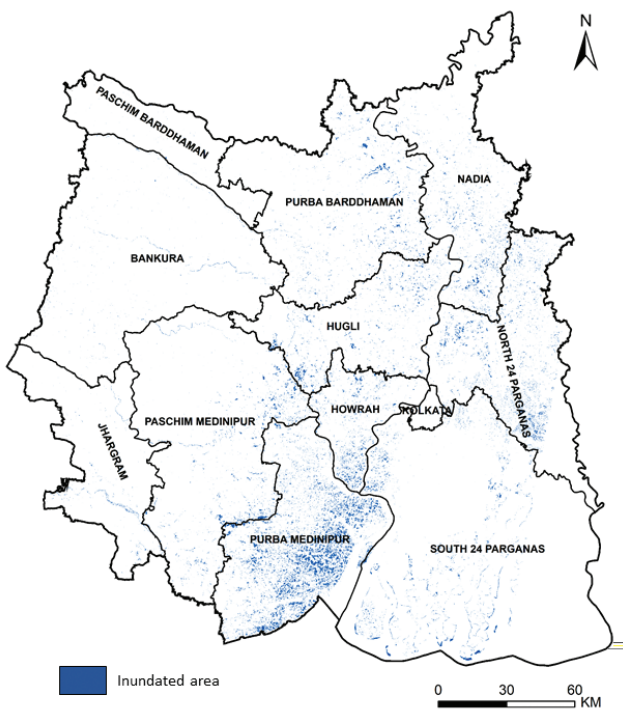


Fig. 5. Spatial distribution of inundated area in the study area

permanent waterbodies were excluded by subtracting the pre-cyclonic imagery from post-cyclonic imagery. It was observed that among the inundated agricultural areas, the standing crops including both growing and matured were in significant proportions (Fig. 6). The estimated agricultural areas under standing crop and matured crop in the field, and land after crop harvest were 20,675 ha, 23,632 ha and 29,283 ha, respectively. The inundated agricultural classes under the different categories are varying from one district to another. The area under inundated agricultural area was insignificant over Kolkata. The area under crop inundation was highest in Purba Medinipur (32,550 ha), where the maximum crop area was harvested, followed by crops at the growing stage. It was observed that the cyclone Amphan had a significant impact on agricultural areas in districts like Purba Medinipur, Nadia, Hugli, Purba Bardhaman, North 24 Parganas, South 24 Parganas and Howrah.

Some field-based information, distributed across different parts of the study area, was collected through AICRPM-NICRA Project (Mohanpur Centre), for validation of the present approach. The details of the ground truth points are given in Table 3. It was found that the proposed approach was able to detect the crop conditions existing during the pre-cyclonic period (Fig. 7a & b). Hence, the same methodology may be adopted for assessing the crop damages caused due to cyclone induced inundation.

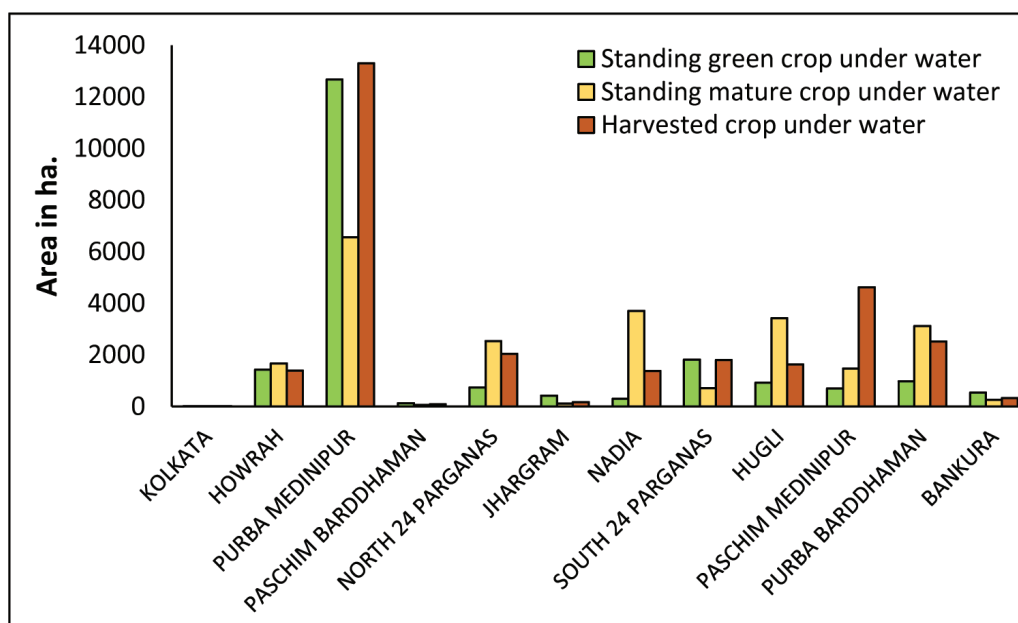
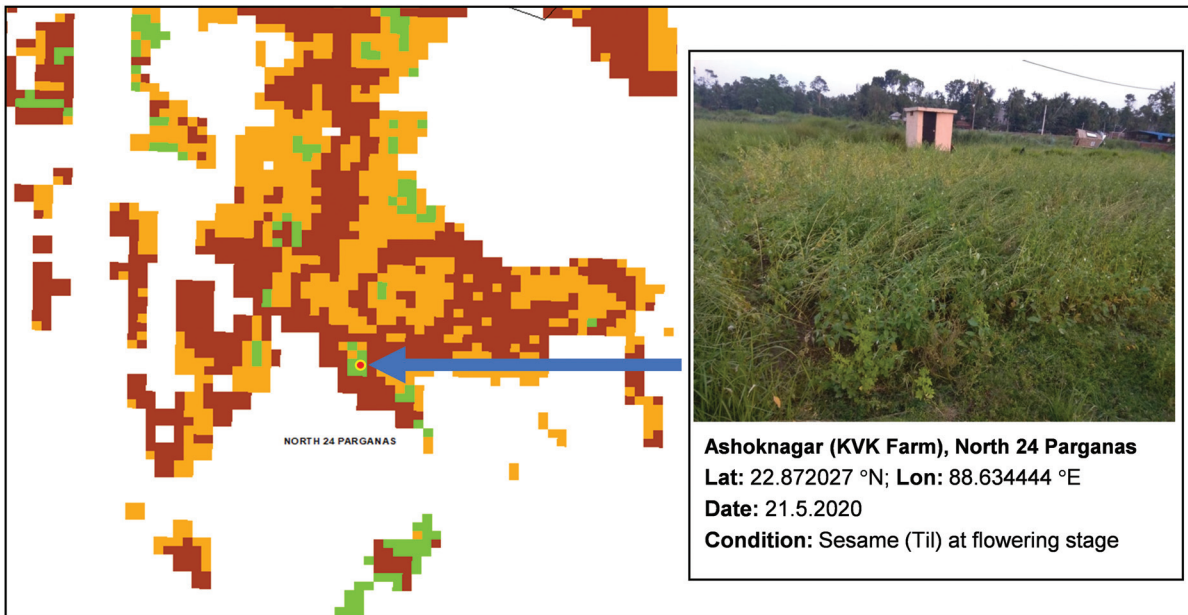


Fig. 6. Inundated agricultural area (in ha.) in different districts

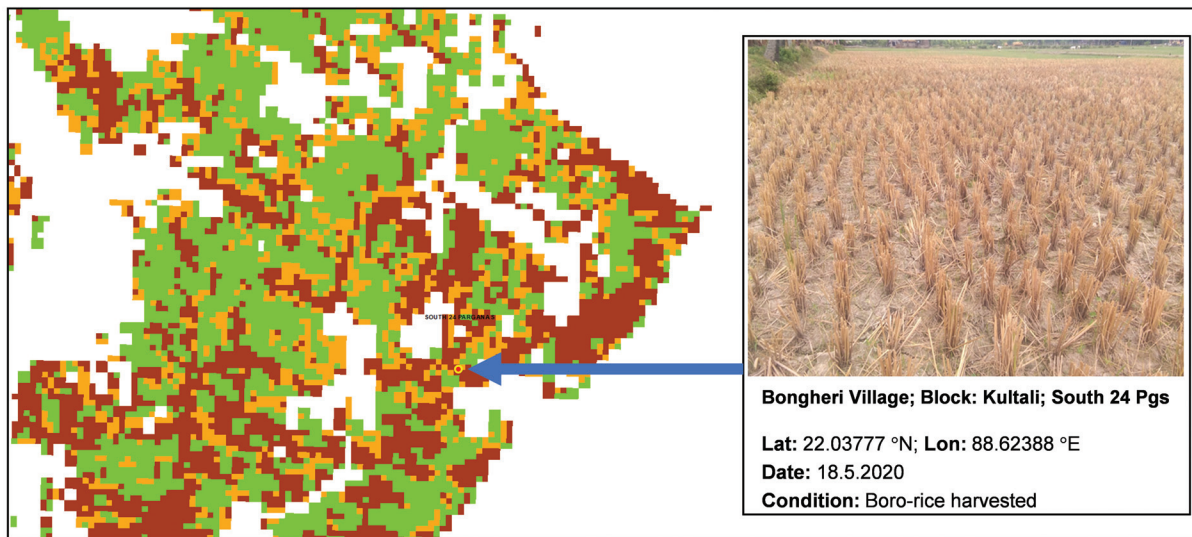
Table 3. Ground based crop information during cyclone Amphan

Sl. No.	Name of location	Geographical coordinates	Crop condition during Amphan	Observations in satellite driven approach
1	Ashoknagar (KVK Farm), North 24 Parganas	22°52'19.3" N 88°38'05.50" E	Sesame at flowering stage	Standing green crop
2	Bongheri village, South 24 Parganas	22°02'16" N 88°37'26" E	Boro rice harvested	Harvested crop
3	Chandamari village, Nadia	23°00'24.88" N 88°29'25.80" E	Standing Brinjal (lodged by cyclone)	Standing green crop
4	Akshyanagar village, South 24 Parganas	22°40'38.95" N 88°18'33.27" E	Boro rice harvested	Harvested crop
5	Kalitala Para, Nadia	23°00'25.89" N 88°27'26.38" E	Jute at knee high stage. (slightly lodged, but ultimately revived)	Standing green crop
6	Chandamari, Nadia	22°59'59.67" N 88°27'30.92" E	standing Cucumber crop, (damaged)	Standing green crop
7	Purba Medinipur	21°59'38.53" N 87°51'44.52" E	Boro rice harvested	Harvested crop
8	Haringhata Block, Nadia	22°54'20.35" N 88°38'10.27" E	Standing pointed gourd crop (damaged)	Standing green crop
9	Purba Medinipur	22°00'50.74" N 87°52'55.56" E	Boro rice harvested	Harvested crop
10	Gontra, Nadia	23°01'03.76" N 88°35'04.14" E	Sesame crop (totally damaged)	Standing green crop
11	Kundakhali, South 24 Pgs	22°06'03.24" N 88°34'57.72" E	Boro rice harvested	Harvested crop



■ standing green crop under water ■ standing mature crop under water ■ harvested crop under water

Fig. 7a. Crop condition existing during pre-cyclonic period over site-1



■ standing green crop under water ■ standing mature crop under water ■ harvested crop under water

Fig. 7b. Crop condition existing during pre-cyclonic period over site-2

Amphan cyclone is one of the severe cyclones which made huge destruction in West Bengal in terms of water inundation, damage to standing crops and houses, and uprooting of many trees. The post-cyclone water inundation was highest in Purba Medinipur. Among the inundated agricultural area, the standing crop including both growing and mature was significant, i.e., 65-90% of the total agricultural area. The proposed methodology could be able to detect the crop conditions that prevailed during the cyclone Amphan, and based on that the vulnerability of the crop damages could be assessed. This is a preliminary study, mainly based on the satellite derived observations. However, the impact assessment can be improved by addressing other factors, like duration and depth of water inundation, types and phenological stages of the crops, presence of harvested crop in the field before threshing, etc. More ground-based information will definitely help in drawing inference on the impact of cyclone Amphan on agricultural areas over West Bengal.

CONFLICTS OF INTEREST

There is no conflict of interest.

ACKNOWLEDGEMENT

The authors are thankful to Dr. Raj Kumar, Director, NRSC, Hyderabad, Dr. C.S. Jha, CGM (RCs) and Dr. D. Dutta, GM, RRSC-East, Kolkata for their continuous support and encouragement during the investigation. The authors acknowledge the support received from Smt. Sharmistha B Pandey and Smt. Nivedita Sinha during satellite data processing. We duly acknowledge the NASA/USGS and ESA for providing Landsat and Sentinel data, respectively. We are also thankful to AICRPM-NICRA Project, Mohanpur Centre for providing ground-based crop information.

REFERENCES

- Clement, M.A., Kilsby, C.G. and Moore, P. (2018). Multi-temporal synthetic aperture radar flood mapping using change detection. *Journal of Flood Risk Management* **11**: 152-168.
- Das, G.K. (2020). Amphan - Maiden Super Cyclone of the Century. *Frontier*. <https://www.frontierweekly.com/views/may-20/25-5-20-Amphan-MaidenSuperCycloneoftheCentury.html>
- DeVries, B., Huang, C., Armston, J., Huang, W., Jones, J.W. and Lang, M.W. (2020). Rapid and robust monitoring of flood events using Sentinel-1 and Landsat data on the Google Earth Engine. *Remote Sensing of Environment* **240**: 111664.
- Dumitru, C.O., Cui, S., Faur, D. and Datcu, M. (2015). Data analytics for rapid mapping: Case study of a flooding event in Germany and the tsunami in Japan using very high-resolution SAR images. *IEEE Journal of Selected Topics in Applied Earth Observations and Remote Sensing* **8**: 114-129.
- Ezzine, A., Saidi, S., Hermassi, T., Kammessi, I., Darragi, F. and Rajhi, H. (2020). Flood mapping using hydraulic modeling and Sentinel-1 image: Case study of Medjerda Basin, northern Tunisia. *The Egyptian Journal of Remote Sensing and Space Sciences* **23**(3): 303-310.
- Fillipponi, F. (2019). Sentinel-1 GRD preprocessing workflow. *Proceedings* **18**(11). <https://doi.org/10.3390/ECRS-3-06201>
- Hoque, R., Nakayama, D., Matsuyama, H. and Matsumoto, J. (2011). Flood monitoring, mapping and assessing capabilities using RADARSAT remote sensing, GIS and ground data for Bangladesh. *Natural Hazards* **57**: 525-548.
- Houghton, J.T., Ding, Y., Griggs, D.J., Noguer, M., van der Linden, P.J. and Xiaosu, D. Eds. (2001) *Climate Change 2001: The Scientific Basis*. Contribution of Working Group I to the Third Assessment Report of the Intergovernmental Panel on Climate Change. Cambridge Univ. Press, Cambridge, U.K. 944 p.
- Islam, A.S., Bala, S.K. and Haque, M.A. (2010). Flood inundation map of Bangladesh using MODIS time series images. *Journal of Flood Risk Management* **3**: 210-222.
- Mitra, A., Dutta, J., Mitra, A. and Thakur T. (2020). Amphan supercyclone: A death knell for Indian Sundarbans. *eJournal of Applied Forest Ecology* eJAFE8141-48.
- Musa, Z.N., Popescu, I. and Mynett, A. (2015). A review of applications of satellite SAR, optical, altimetry and DEM data for surface water modeling, mapping and parameter estimation. *Hydrology and Earth System Sciences* **19**: 3755-3769.

- Nandi, I., Srivastava, P.K. and Shah, K. (2017). Floodplain mapping through support vector machine and optical/infrared images from Landsat 8 OLI/TIRS sensors: Case study from Varanasi. *Water Resources Management* **31**: 1157-1171.
- Notti, D., Giordan, D., Caló, F., Pepe, A., Zucca, F. and Galve, J.P. (2018). Potential and limitations of open satellite data for flood mapping. *Remote Sensing* **10**: 1673.
- Sajjad, A., Lu, J., Chen, X., Chisenga, C., Saleem, N. and Hassan, H. (2020). Operational monitoring and damage assessment of riverine flood-2014 in the lower Chenab plain, Punjab, Pakistan, using remote sensing and GIS techniques. *Remote Sensing* **12**: 714. <https://doi.org/10.3390/rs12040714>
- Sarker, C., Mejias, L., Maire, F. and Woodley, A. (2019). Flood mapping with convolutional neural networks using spatio-contextual pixel information. *Remote Sensing* **11**: 2331.
- Solomon, S., Qin, D., Manning, M., Marquis, M., Averyt, K., Tignor, M.M.B., Miller Jr., H.L. and Chen, Z. (2007). *Climate Change 2007: The Physical Science Basis*. Contribution of Working Group I to the Fourth Assessment Report of the Intergovernmental Panel on Climate Change. Cambridge Univ. Press, Cambridge, U.K. 996 p.